



## FLOW VISUALIZATION OF THE WIND FIELD IN URBAN STREET CANYONS WITH DIFFERENT BUILDING ARCHITECTURE

**João Carlos Fernandes de Queiroz**

**Bianca Hulle de Souza**

Mechanical Technical Department, IFES, Vitória, E.S., Brazil

jcqueiroz@hotmail.com

biancahulles@hotmail.com

**Daniel Zandonade Matta**

Civil Technical Department, IFES, Vitória, E.S., Brazil

danielzandonade1@hotmail.com

**Reginaldo Rosa Cotto de Paula**

Sanitary and Environmental Engineering Department, IFES, Vitória, E.S., Brazil

cottoreginaldo@gmail.com

**Marcos Sebastião de Paula Gomes**

Mechanical Engineering Department, PUC-Rio, Rio de Janeiro, R.J., Brazil

mmsgomes@mec.puc-rio.br

**Abstract.** *In this paper experimental investigations of the wind flow in an idealized urban environment are presented. The aim was to evaluate the effect of building geometry and surround blockage on the natural ventilation system in urban street canyons. Two different urban street canyon architectures were represented by cubical and rectangular scale model buildings of the same size and height. These scale model buildings were arranged in a symmetric configuration with different separation distances and two wind speeds. The experiments were conducted in an atmospheric boundary layer wind tunnel. The smoke injection technique was used to investigate the vortex system of the flow around the buildings. The results of visualizations of the flow show that wind field was strongly influenced by the flow structure.*

**Keywords:** *urban street canyon, flow visualization, wind tunnel experiments*

### 1. INTRODUCTION

Information about the wind flow characteristic over buildings is necessary for design of natural ventilation systems in urban regions. The complexity of wind-structure interaction depends on various parameters, such as approach wind flow, vortical flow patterns generated around a structure, the flow separation, the vortex formation and wake development. Various studies on flow around buildings in recent years have focused of the flow patterns that develop around individual buildings (Lakehal and Rodi, 1997; Tominaga and Stathopoulos, 2010; Burgo *et al.*, 2012). However, most buildings are situated in urban regions, in which the superposition and interaction of flow patterns are [influenced by] adjacent buildings and other structures.

Many urban regions suffer from poor ventilation systems and air quality problems due to improper urban planning. Sources of pollutants situated within a street canyon (vehicle emissions) or close to the roof-level (stacks) associated with rapid development of urban activities consequently result in air quality degradation (Chan *et al.*, 2003).

Since urban flow is dominated by interactions of oncoming wind fields and surrounding buildings, it is not easy to arrive at a general formula to describe a wind field for a particular canyon geometry for application in urban design due to various interdependent factors (Chan *et al.*, 2003). For example, one of the most important parameters that govern the wind flow in urban street canyons is the physical layout, which includes building geometry, architectural design, and dimensioning of the street canyon itself (Yassin, 2011). Therefore, study in this area is necessary to evaluate the influence of street canyon architecture upon these phenomena and to provide up to date reference data for urban planning.

This has involved experimental and numerical observations of the flow regimes of complex morphology of an urban street canyon. When the wind is perpendicular to the street there are three flow regimens as function of building (length-to-depth ratio) and canyon (depth-to-width ratio) in the corridor between two rows of similar height buildings (Oke, 1988; Hunter *et al.*, 1992; Louka *et al.*, 1988): (1) isolated roughness flow: this flow regime develops when the building height to street width ratio,  $H/W$  is less 0.3, for widely spaced building the flow returns to the upwind before downwind building is encountered. This is similar to the flow which develops around an isolated building; (2) wake interference flow: when the building are more closely spaced,  $0.3 < H/W < 0.65$ , the downwind building disturbs the flow before readjustment can take place; (3) skimming flow: this flow regime develops when  $H/W > 0.65$ . This flow is

characterized by a vortex within the canyon, which has found been not to exceed the building height. This is a usual flow regime encountered in a city center.

Since the building design may cause effects on the flow regimes, the purpose of this paper is to investigate experimentally the influence of  $H/W$  ratios on the ventilation system of urban street canyons. Wind tunnel experiments have been performed to evaluate the flow in an idealized urban environment of cubical and rectangular buildings immersed in a neutral atmospheric boundary layer.

## 2. MATERIAL AND METHODS

The flow considered in this work was investigated in an open return wind tunnel with a test section 2.0 m long, 0.5 high and 0.5 wide, in the Energy Laboratory of IFES, Vitoria, Brazil. An atmospheric boundary layer (ABL) was developed in the wind tunnel working section, with characteristics representative of neutral atmospheric conditions. The ABL with  $\delta = 0.3$  m deep was generated by various spires and roughness elements made with wood that were installed upwind of the test area of the wind tunnel. The dimensions and spacing of spires and roughness elements were calculated using the methodology proposed by Irwin (1981). The mean streamwise velocity has the following power law profile:

$$\frac{U(z)}{U_\delta} = \left( \frac{z}{\delta} \right)^p \quad (1)$$

The velocity profile was fitted with  $p = 0.30$  which corresponds to the velocity profile over a suburban site (Blessman, 1988). To study the effects of ambient wind on flow in urban areas, two kinds of obstacles were considered in the wind tunnel experiments: two row with six cubical buildings of  $H = 0.08$  m, Fig. 1 and two row with six prismatic rectangular buildings with a height of  $0.16$  ( $2H$ ), Fig. 2, where  $H$  is the height of the obstacle cube. These scale model buildings were arranged in a symmetric configuration with three different separation distances between buildings ( $W_2$ ) and using two wind speeds. In all experiments the street width ( $W_1$ ) was of the same value as the cube height. The main street was parallel to the oncoming wind flow and the spacing between the buildings was perpendicular to it.

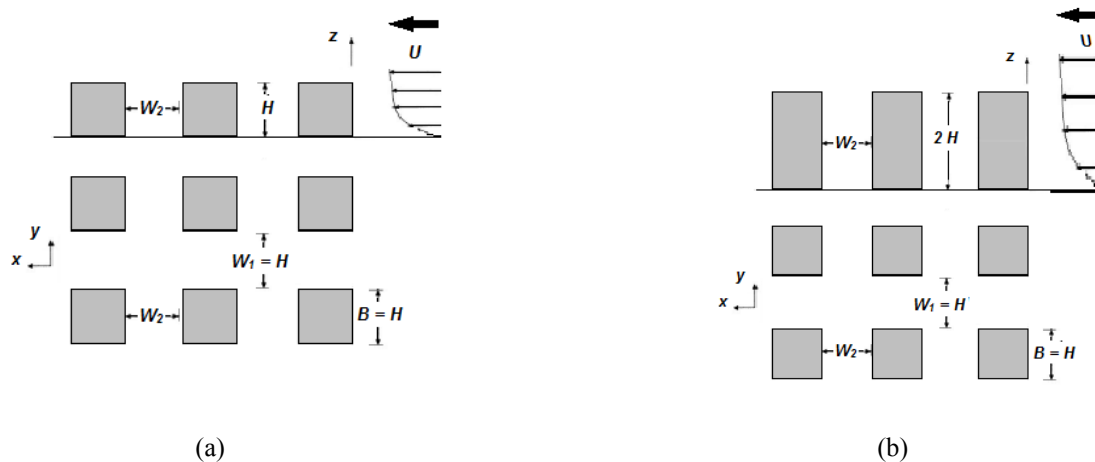


Figure 1. Schematic of urban street-canyon model arrangement: (a) cubical buildings and (b) prismatic rectangular buildings.

Smoke flow technique was used to visualize the wind flow around the six buildings in the urban street-canyons. Fluid from a smoke machine (LASER DJ 1500w) was generated and emitted into the wind tunnel through a pipe (50 mm diameter), with the outflow downstream of the urban region. A green laser light passing through a spinning cylindrical lens was used to illuminate the vicinity of the buildings to facilitate a clear visualization of the vortex system for analysis of the wind flow. A 500 mW (532 nm) diode laser module was mounted outside of the wind tunnel in the center line at an elevation of 1.7 cm.

A digital camera (Fujifilm HS 10) operating at a speed of the 240 frames per second (fps) was used to record the smoke patterns. The camera was placed outside the wind tunnel on either side looking through the side. Selected sequences of video pictures were studied both digitally and visually. In this work the Reynolds numbers were based on building height and wind velocity at the building height,  $U_h$ . In addition air density of  $1.185 \text{ kg/m}^3$  and air viscosity of  $1.82 \times 10^{-5} \text{ kg/m}^2 \cdot \text{s}$  were used.

### 3. RESULTS

Six cases with different building aspect ratios and two wind velocities were simulated and analyzed experimentally. The direction of wind was to perpendicular to the frontal surface of the obstacles.

#### 3.1 Cubical Buildings: Incident Region

Figures 2, 3 and 4 show the flow patterns on the  $x-z$  plane in the incident region of cubical buildings corresponding to  $H/W_2 = 1.0$ , 0.67 and 0.5, respectively. When wind flow approaches the building and impinges on the frontal face, part of the flow goes toward the ground and returns in the opposite direction to the main flow. In front of the obstacle due to the interaction between the incident and reverse flow, the formation of standing vortex occurred near the ground and below the stagnation point. Despite the different building spacing's, the patterns of the recirculation region upstream of obstacles were very similar to each other. The flow pattern was characterized by a separation region with its reattachment point on the top surface of first building in urban region, as shown in Fig. 3-(A), 3-(B) and 4-(B).

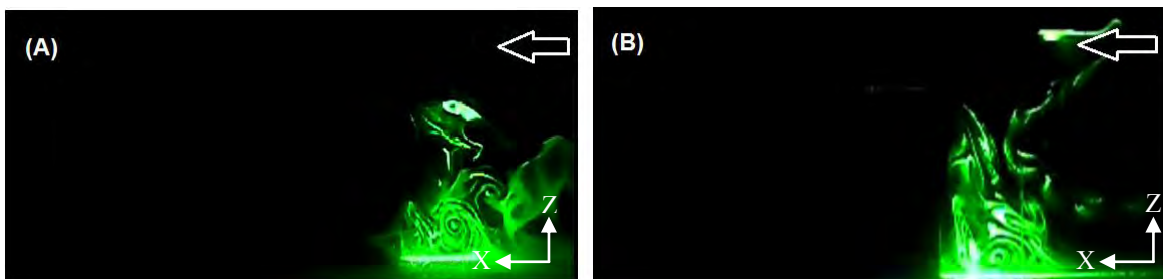


Figure 2. Side view of incident region around cubical buildings ( $H/W_2 = 1.0$ ): (A)  $Re = 1379$  and (B)  $Re = 2913$ .

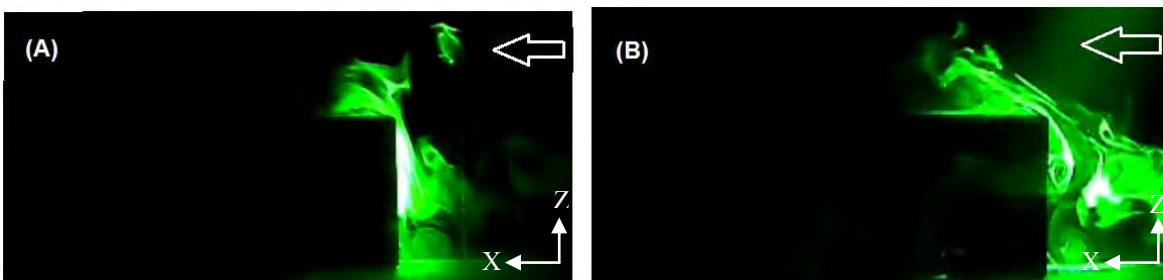


Figure 3. Side view of incident region around cubical buildings ( $H/W_2 = 0.67$ ): (A)  $Re = 1379$  and (B)  $Re = 2913$ .

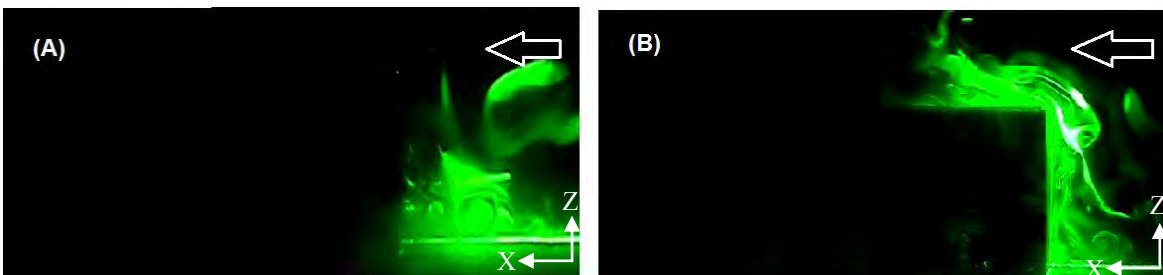


Figure 4. Side view of incident region around cubical buildings ( $H/W_2 = 0.5$ ): (A)  $Re = 1379$  and (B)  $Re = 2913$ .

#### 3.2 Cubical Buildings: Flow Pattern Between Buildings

Figures 5 and 6 show the flow patterns on the  $x-z$  plane corresponding to  $H/W_2 = 1.0$ , within the canyon between the first and second buildings and second and third buildings, respectively. In both cases the formation of one counterclockwise rotating vortex was observed see Fig. 5. The vortex circulation between the buildings is known as skimming flow as described by Oke (1988). Figure 7 shows that within the space between the second and third buildings there was generated a complex pattern of rotating vortices toward the frontal face and near the ground of the downwind building.

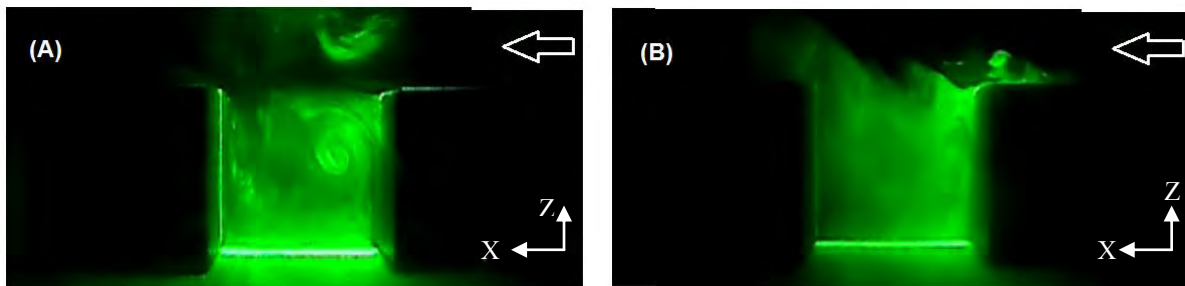


Figure 5. Side view of flow visualization within canyon between first and second buildings ( $H/W_2 = 1.0$ ): (A)  $Re = 1379$  and (B)  $Re = 2913$ .

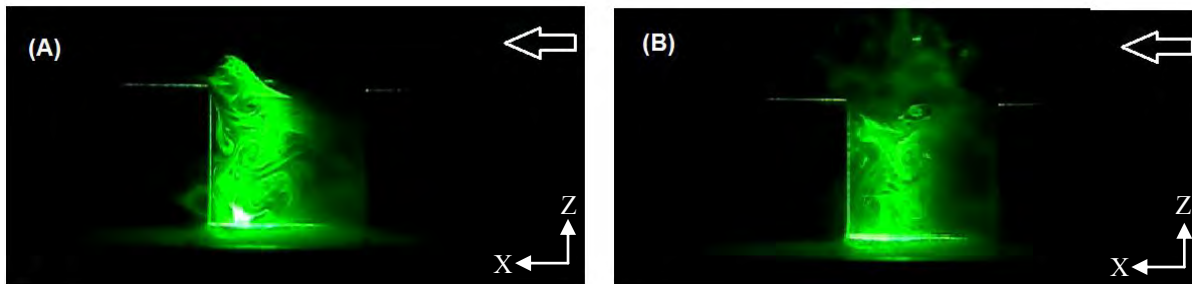


Figure 6. Side view of flow visualization within canyon between second and third buildings ( $H/W_2 = 1.0$ ): (A)  $Re = 1379$  and (B)  $Re = 2913$ .

Figures 7 and 8 show the flow patterns on the  $x - z$  plane corresponding to  $H/W_2 = 0.67$  within the canyon between the first and second buildings and second and third buildings, respectively. As the canyon opening increases were generated a double rotating vortex developed toward the lee wall of the upstream. The results of flow visualization suggested that this behavior was due to the transition from skimming to wake interference flow.

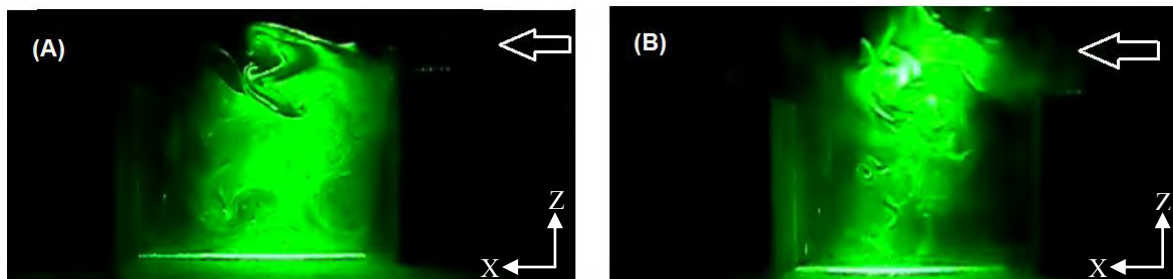


Figure 7. Side view of flow visualization within canyon between first and second buildings ( $H/W_2 = 0.67$ ): (A)  $Re = 1379$  and (B)  $Re = 2913$ .

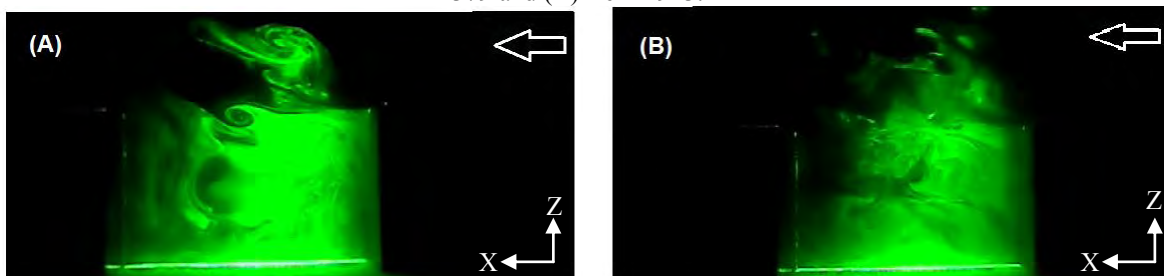


Figure 8. Side view of flow visualization within canyon between second and third buildings ( $H/W_2 = 0.67$ ): (A)  $Re = 1379$  and (B)  $Re = 2913$ .

Figure 9 and 10 show the flow patterns corresponding to  $H/W_2 = 0.5$ , within the canyon between the first and second buildings and second and third buildings, respectively. The results showed a strong vortex circulation with the large roll vortex system. Small vortices were observed at the leeward face of upwind building, but they were not dominant. This flow regime presented characteristics of wake interference flow as described by Oke (1988).

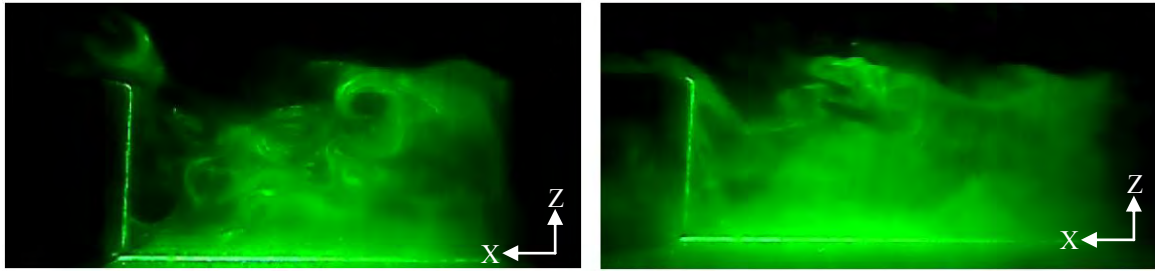


Figure 9. Side view of flow visualization within canyon between first and second buildings ( $H/W_2 = 0.5$ ): (A)  $Re = 1379$  and (B)  $Re = 2913$ .

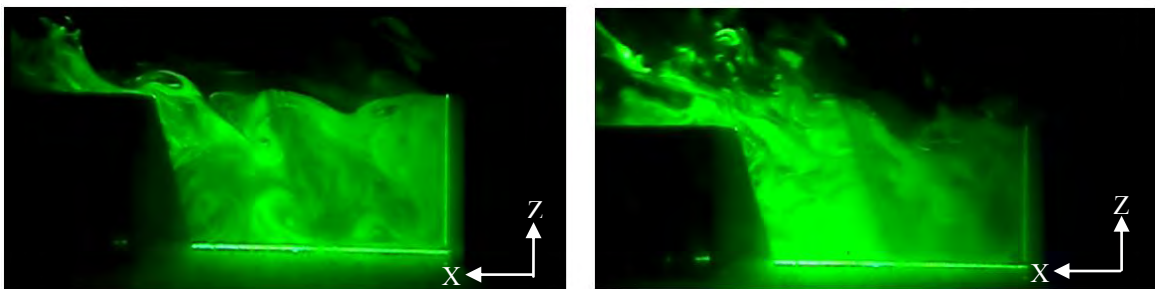


Figure 10. Side view of flow visualization within canyon between second and third buildings ( $H/W_2 = 0.5$ ): (A)  $Re = 1379$  and (B)  $Re = 2913$ .

### 3.3 Cubical Buildings: Flow Patterns in the Wake of Last Buildings

Figures 11, 12 and 13 show the flow structure in the near wake of the last cubical building corresponding to  $H/W_2 = 1.0$ ; 0.67 and 0.5, respectively. The wake vortex structure behind the third building can be clearly identified. The recirculation zone of the wake extends above the level of the top of the last building. From flow visualization was possible to capture the vortex-shedding phenomenon. In all experiments with different aspect ratios the flow in the near wake presents a similar pattern.

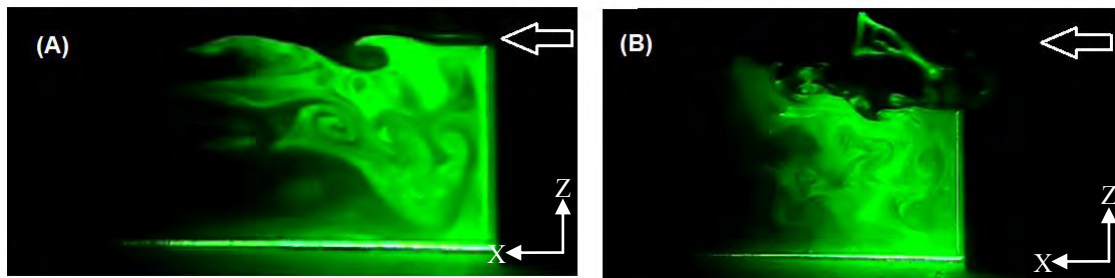


Figure 11. Side view of flow visualization in the near wake of last building ( $H/W_2 = 1.0$ ): (A)  $Re = 1379$  and (B)  $Re = 2913$ .

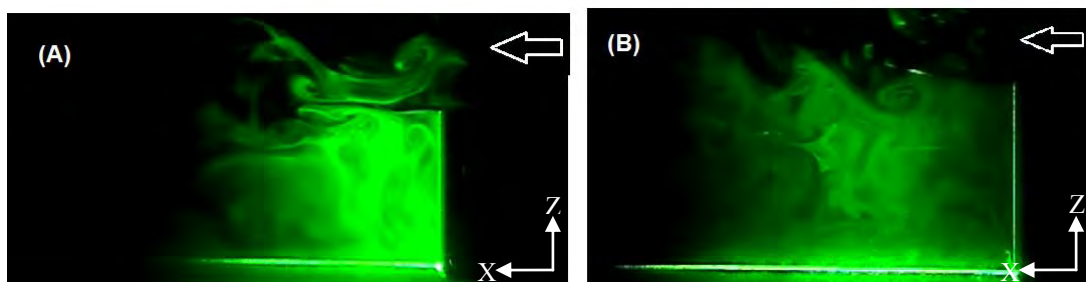


Figure 12. Side view of flow visualization in the near wake of last building ( $H/W_2 = 0.67$ ): (A)  $Re = 1379$  and (B)  $Re = 2913$ .

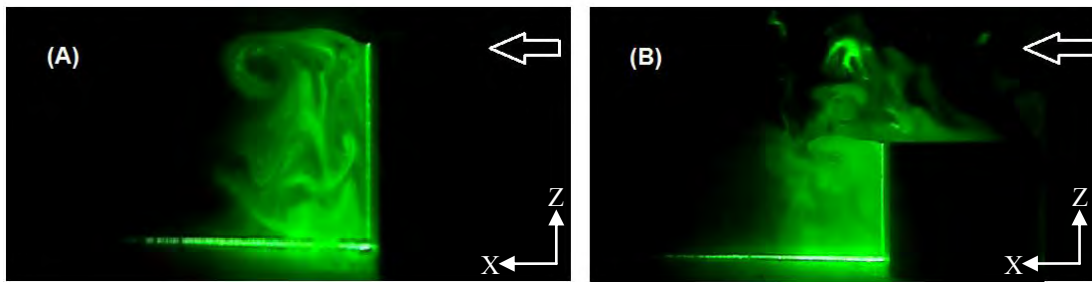


Figure 13. Side view of flow visualization in the near wake of last building ( $H/W_2 = 0.5$ ): (A)  $Re = 1379$  and (B)  $Re = 2913$ .

### 3.4 Prismatic Rectangular Buildings: Incident Region

Figures 14, 15 and 16 show flow characteristics qualitatively in the incident region of the prismatic rectangular buildings for the aspect ratios  $H/W_2 = 2.0$ ; 1.33 and 0.5, respectively. The results of flow visualization show that wind was first displaced upstream when approaching the building array. On the frontal face of the first building the wind was blocked and there was standing vortex formation in front of the windward wall of the rectangular building in all aspect ratios investigated in the present work.

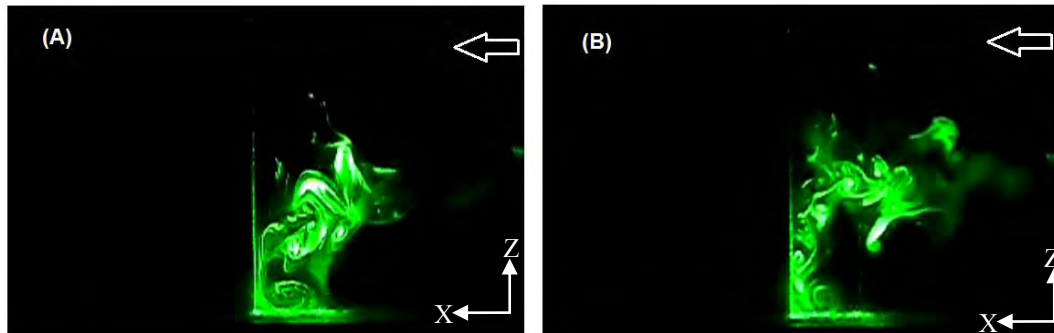


Figure 14. Side view of incident region of the rectangular buildings ( $H/W_2 = 2.0$ ): (A)  $Re = 3747$  and (B)  $Re = 7803$ .

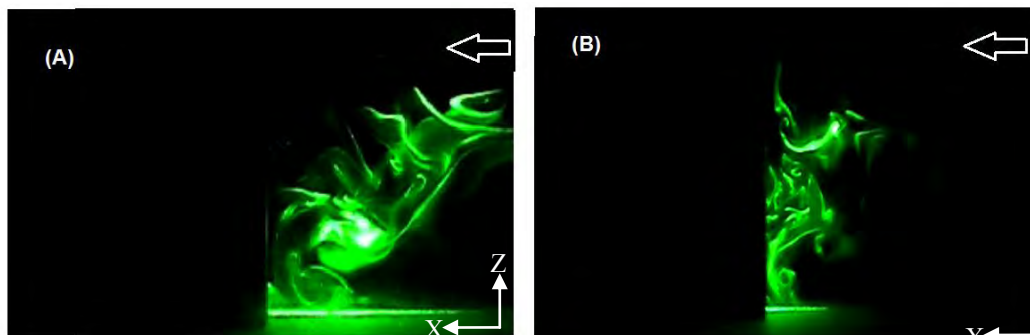


Figure 15. Side view of incident region of the rectangular buildings ( $H/W_2 = 1.33$ ): (A)  $Re = 3747$  and (B)  $Re = 7803$ .

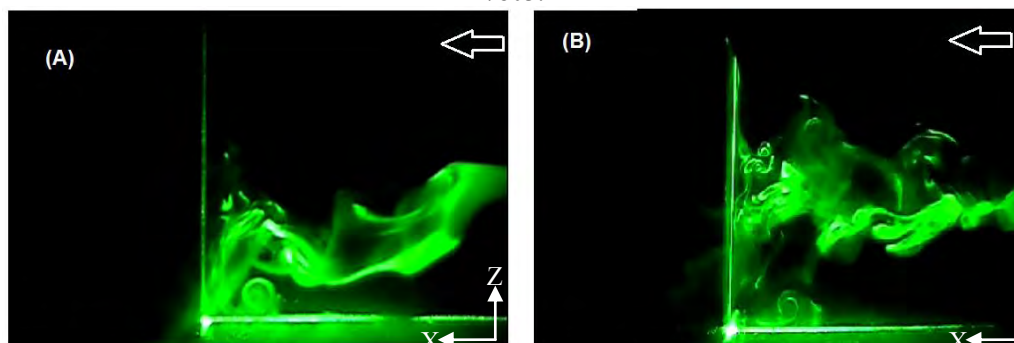


Figure 16. Side view of incident region of the rectangular buildings ( $H/W_2 = 0.5$ ): (A)  $Re = 3747$  and (B)  $Re = 7803$ .

### 3.5 Prismatic Rectangular Buildings: Flow Pattern Between Buildings

Figures 17 and 18 show the flow patterns on the  $x-z$  plane, around prismatic rectangular obstacles corresponding to  $H/W_2 = 2.0$ , within the canyon between the first and second buildings and second and third buildings, respectively. Figures 19 and 20 show the flow patterns around rectangular obstacles with  $H/W_2 = 1.33$ , within the canyon between the first and second buildings and second and third buildings, respectively. Qualitatively it was observed that the sheltering effect of tall buildings produced weak winds in the narrow canyon spacing. The flow separation on the leeward wall of the upstream building generated turbulent recirculation flow immediately downstream with various counterclockwise and clockwise rotating vortices.

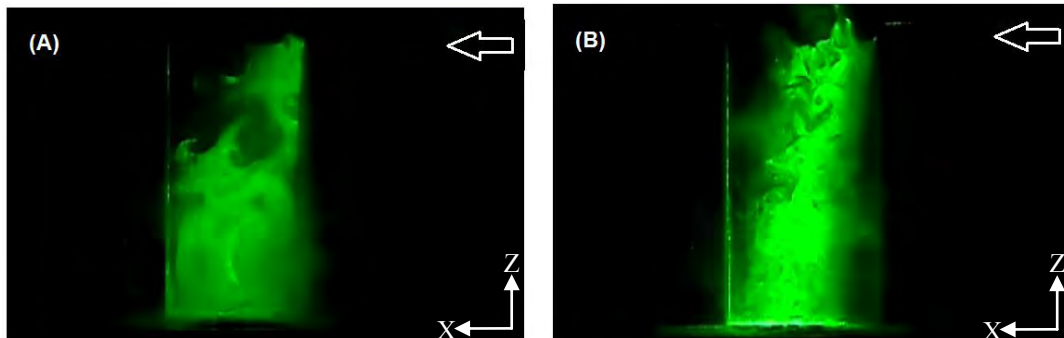


Figure 17. Side view of flow visualization within canyon between first and second buildings ( $H/W_2 = 2.0$ ): (A)  $Re = 3747$  and (B)  $Re = 7803$ .

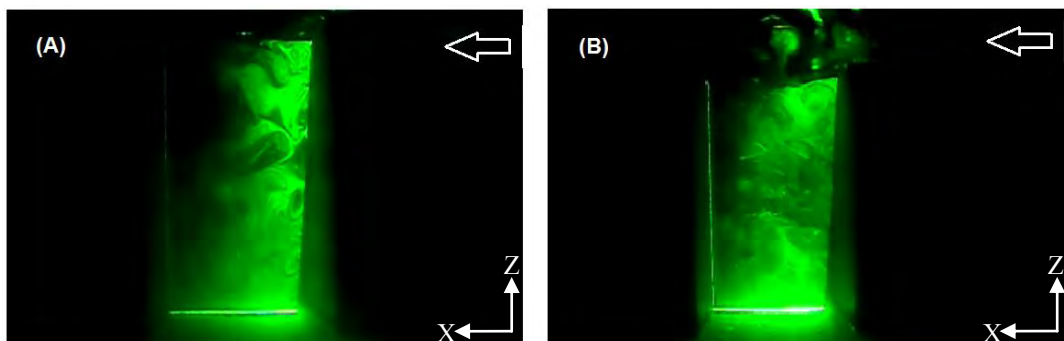


Figure 18. Side view of flow visualization within canyon between second and third buildings ( $H/W_2 = 2.0$ ): (A)  $Re = 3747$  and (B)  $Re = 7803$ .

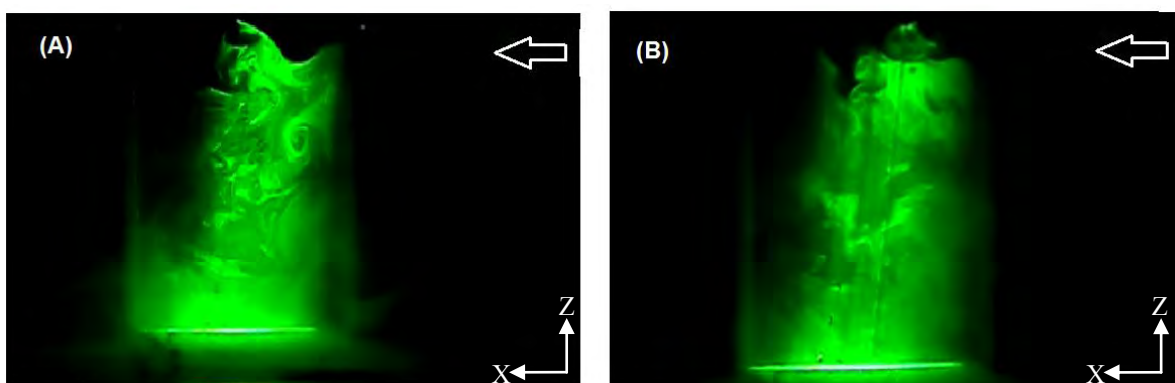


Figure 19. Side view of flow visualization within canyon between first and second buildings ( $H/W_2 = 1.33$ ): (A)  $Re = 3747$  and (B)  $Re = 7803$ .

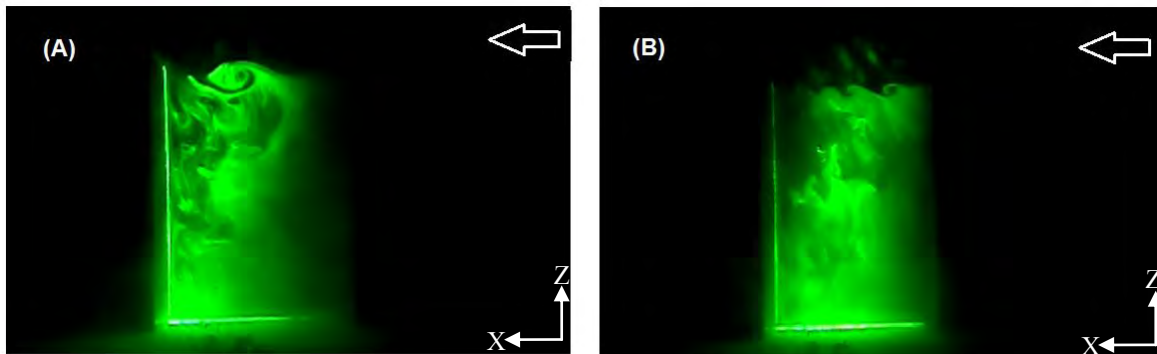


Figure 20. Side view of flow visualization within canyon between second and third buildings ( $H/W_2 = 1.33$ ): (A)  $Re = 3747$  and (B)  $Re = 7803$ .

Figures 21 and 22 show the flow patterns on the  $x - z$  plane, around prismatic rectangular obstacles corresponding to  $H/W_2 = 0.5$ , within the canyon between the first and second buildings and second and third buildings, respectively. The flow visualization showed the increasing complexity of the wind flow with increasing canyon spacing. A large rotating roll vortex occurred within the building spacing and was driven, by the flow, toward downwind building. At the level of the top the upstream obstacle vortex shedding was observed.

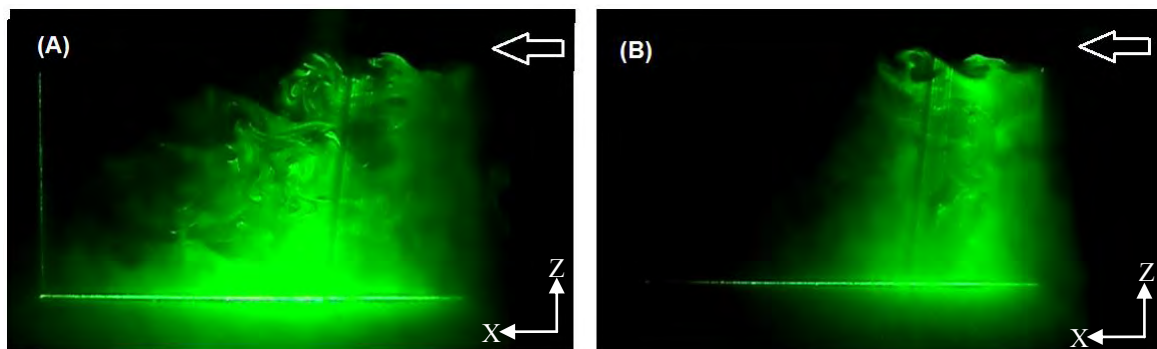


Figure 21. Side view of flow visualization within canyon between first and second buildings ( $H/W_2 = 0.5$ ): (A)  $Re = 3747$  and (B)  $Re = 7803$ .

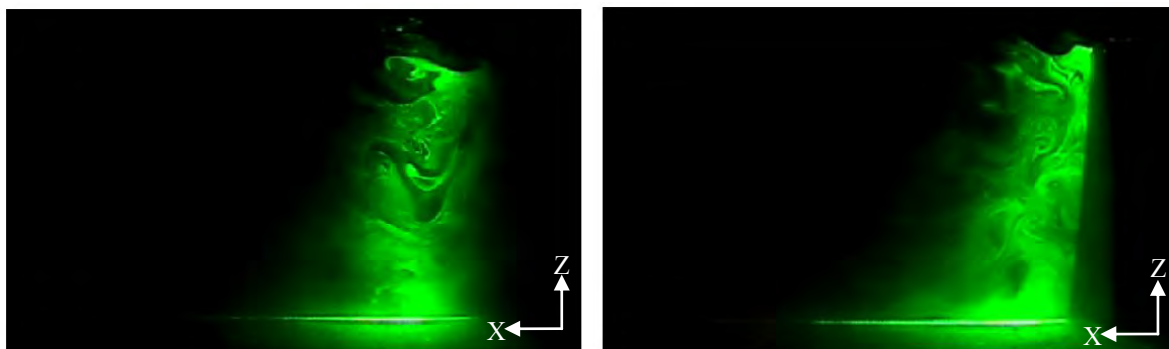


Figure 22. Side view of flow visualization within canyon between second and third buildings ( $H/W_2 = 0.5$ ): (A)  $Re = 3747$  and (B)  $Re = 7803$ .

Figures 23 shows the normalized mean wind vertical profile measured in the center line of the street canyon ( $y/H_b = 0$ ) and roof of buildings ( $y/H_b = 1.0$ ) corresponding to  $H/W_2 = 0.5$  at the cubical buildings ( $H_b = 0.08\text{m}$ ). The results showed wind velocity was accelerated at  $x/H_b = 3.5$  in the in the range  $0.0 < z/H_b < 1.0$ , but the wind flow reached an equilibrium condition at  $x/H_b = 6.5$  and  $9.5$ , see Fig. 23(a). The profiles indicate that there is not significant influence of the buildings on the wind speed on the roof, see Fig. 23(b).



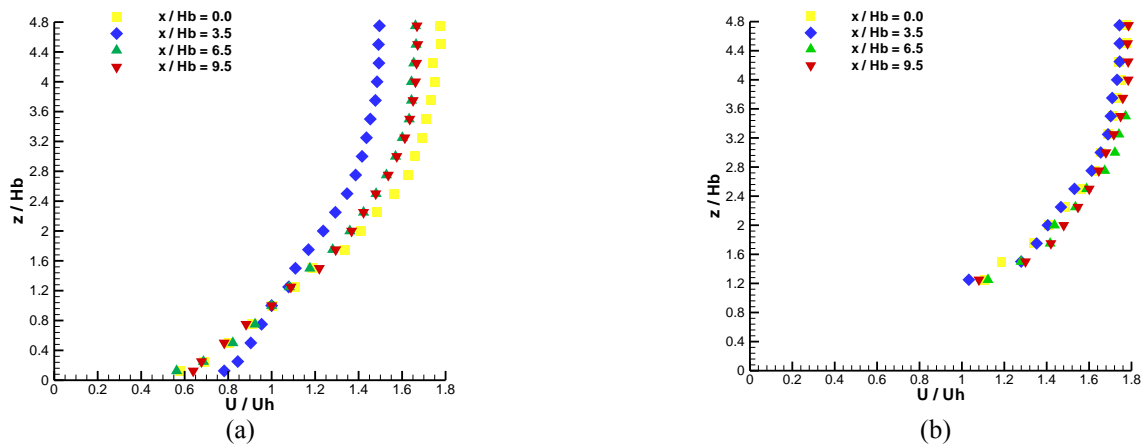


Figure 23 – Normalized mean wind vertical profile in the street canyon formed by cubical buildings at  $H_b/W_2 = 1.0$ : (a) center line of street and (b) on the roof of buildings.

Figure 24 shows the normalized mean wind vertical profile ( $U/U_h$ ) measured in the center line of the street canyon and roof of buildings corresponding to  $H_b/W_2 = 2.0$ , at the prismatic rectangular buildings ( $H_b = 0.16$  m). The results showed a retardation of the wind flow in the center of street at  $0.0 < z/H_b < 0.8$ , see Fig. 24(a). The profiles indicate that there is not significant influence of the buildings on the wind speed on the roof, see Fig. 24(b).

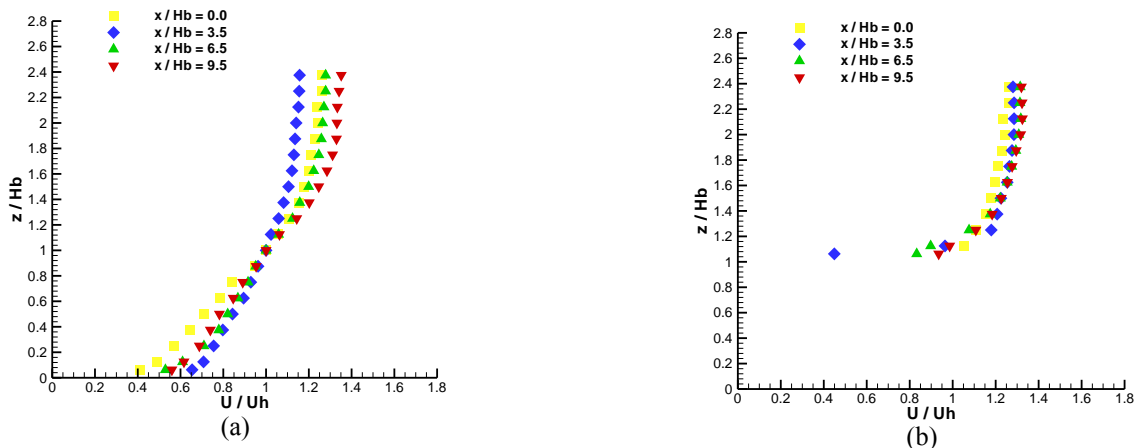


Figure 24 – Normalized mean wind vertical profile in the street canyon formed by prismatic rectangular buildings at  $H_b/W_2 = 1.0$ : (a) center line of street and (b) on the roof of buildings.

#### 4. CONCLUSIONS

Wind tunnel experiments in idealized urban street canyons were carried out with the smoke injection technique. Two different arrangements of urban canyon were formed by six cubical and six rectangular homogeneous buildings. The results presented in this work for flow in idealized urban street canyons were expected to help in analyses of the complexities of turbulent flow in urban regions.

In this work by varying the canyon spacing it was possible to investigate the skimming and wake interference flow when cubical buildings were used. For narrow spacing between cubical buildings ( $H/W_2 = 1.0$ ) there was observed a primary rotating vortex with negative vorticity. The pictures of flow visualization showed that with increasing canyon spacing, the street-canyon rotating vortex increases. These roll vortices presented positive and negative vorticity. The flow patterns around rectangular obstacles showed a shelter effect due to the presence of tall buildings, which produced weak winds in narrow canyon spacing ( $H/W_2 = 2.0$  and  $1.33$ ).

#### 5. ACKNOWLEDGEMENTS

The authors would like to acknowledge the Mechanical Technical Department of IFES, Vitoria, Brazil and the financial support from Council for Scientific and Technological Development (CNPq) and Vale Company.

João Carlos Queiroz, Bianca Hulle de Souza, Daniel Zandonade Matta, Reginaldo Cotto de Paula, Marcos Sebastião de Paula Gomes  
Flow Visualization of the Wind Field in Urban Street Canyons with Different Building Architecture

## 6. REFERENCES

- Blessmann, J., 1988. "O vento na Engenharia Estrutural". Editora Universidade, Universidade Federal do Rio Grande do Sul.
- Burgo, A., Paula, R.R.C, Cezana, F.C., Souza, B.H., Gomes, M.S.P., 2012. "Study of wake region of the typical isolated building. Part I: Flow Visualization". In Proceedings of the 14<sup>th</sup> Brazilian Congress of Thermal Sciences and Engineering – ENCIT2012. Rio de Janeiro, Brazil.
- Chang, C. and Meroney, R.N., 2003. "Concentration and flow distributions in urban street canyons: wind tunnel and computation data". *Journal of Wind Engineering and Industrial Aerodynamics*, Vol. 91, pp. 1141-1154.
- Hunter, L.J., Johnson, G.T., and Watson, I.D., 1992. "An investigation of three-dimensional characteristics of flow regimes within the urban region". *Atmospheric Environment. Part B. Urban Atmosphere*, Vol. 26, pp. 425-432.
- Irwin, H.P., 1981. "The Design of Spires for Wind Simulation". *Journal of Wind Engineering and Industrial Aerodynamics*, Vol. 7, pp. 361-366.
- Lakehal, D. and Rodi, W., 1997. "Calculation of the flow past a surface-mounted cube with two-layer turbulence models". *Journal of Wind Engineering and Industrial Aerodynamics*, Vols. 67/68, pp. 65-78.
- Louka, P., Belcher, S.E. and Harrison, R.G., 1998. "Modified street canyon flow". *Journal of Wind and Engineering and Industrial Aerodynamics*, Vol. 74, pp. 485-493.
- Oke, T.R., 1988. "Street design and urban canopy layer climate". *Energy and Buildings*, Vol. 11, pp. 103-113.
- Tominaga, Y. and Stathopoulos, T., 2010. "Numerical simulation of dispersion around an isolated cubic building: Modelo evaluation of RANS and LES". *Building and Environment*, Vol. 45, pp. 2231- 2239.
- Yassin, M.F., 2011. "Impact of height and shape of building roof on air quality in urban street canyons". *Atmospheric Environment*, Vol. 45, pp. 5220-5229.

## 7. RESPONSIBILITY NOTICE

The authors are the only ones responsible for the printed material included in this paper.